Indonesian Journal of Physics
Vol. 34. No.2, 25 December 2023
Journal homepage: http://ijphysics.com

Design of Neutron Activation and Radiography Facilities Based on DD Generator

Dian Adi Prastowo[1*]
[1]*Research Center for Radiation Detection and Nuclear Analysis Technology, BRIN*
Jalan Raya Puspiptek, South Tangerang 15314, Indonesia

(Received: 29 September 2023, Revised: 23 December 2023, Accepted: 27 December 2023)

Abstract

Deuterium-deuterium neutron generator works by fusing two deuterons to produce fast neutrons at energy 2.45 MeV. The energy must be lowered down until thermal regions so that it can be used for experiments such as neutron activation analysis (NAA) and radiography. In this study, design and simulation of NAA and radiography facilities using DD neutron generator have been conducted by PHITS 3.30 Monte Carlo simulation. A cylindrical DD neutron tube (E = 2.45 MeV isotropic, 5 x 10^9/s flux) is surrounded by high-density polyethylene blocks which serve as the moderator. Within the moderator there are several cavities for NAA experiments. High thermal flux up to 1.95 x 10^9/(cm^2.s) can be achieved at about 20 cm from the source. A 90 cm long beam tube with super mirror layers is then installed either radially or tangentially for radiography purposes. From the simulation, radial beam tube delivers thermal flux of 7.86 x 10^3/(cm^2.s) while tangential beam tube transports 1.86 x 10^3/(cm^2.s). The radial configuration still delivers many fast neutrons but the tangential configuration succeeds in suppressing the number of fast neutrons. This result can serve as a preliminary study for the commissioning of radiation facilities based on compact, low-power neutron source.

Keywords: DD generator, NAA, radiography, PHITS

INTRODUCTION

A deuterium-deuterium (DD) neutron generator is an electronic tube capable of producing neutrons from the fusion reaction of two deuterium nucleus. In 50% probability, the products of this fusion are a helium-3 and a fast neutron with energy of 2.45 MeV [1]. Various researches have been conducted to design or to make use of facilities based on DD neutron generators such as for radioisotope production [2], BNCT radiotherapy [3], prompt gamma activation analysis [4] or fast neutron radiography [5-6].

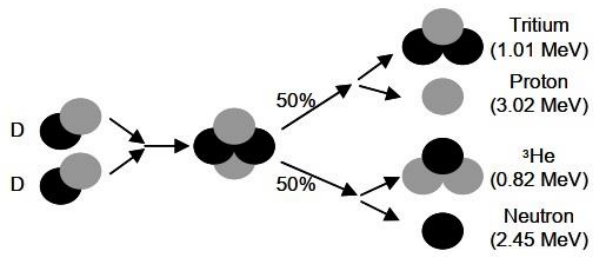

Fig. 1. Fusion reaction of two deuterium nuclei [1]

Small-scale neutron activation analysis generally employs neutrons from radioisotopic sources such as Am-Be of Cf-252 [4]. This can be done due to small thermal flux requirement for activation analysis, which is in the range of 10^7 – 10^8 neutrons/(cm^2.s) per IAEA Reports [7]. However, Am-Be sources have very high gamma background which require more shielding. The energy of Cf-252 source, while milder and more compact, cannot be turned off and thus should be handled with care even when not being worked on. Meanwhile, DD generator is a monoenergetic source that can be switched on and off so that it does not pose hazard present in the isotopic sources. The neutron energy is also lower than deuterium-tritium (DT) generator, another fusion-based source, which is 14.1 MeV so it requires less moderation than DT source [4].

Thermal neutron radiography uses specifically neutrons in the thermal energy range to penetrate objects. The flux recommended by the IAEA is approximately 10^6 neutrons/(cm^2.s) [8-9]. This is however can only be reached by research reactors or spallation sources as the total flux of accelerator-

1* Corresponding author. E-mail address: dian065@brin.go.id

based neutron sources are generally low, especially the portable ones [10-11].

The goal of this research is to investigate the feasibility of DD neutron generator as the source for some nuclear technique experiments such as neutron activation analysis and radiography. These two categories were selected due to their low flux requirement, unlike for elastic or even inelastic scatterings which need bigger flux [12]. The result hopefully could be implemented for the development of compact laboratories that can be utilized for industrial applications and/or educational purposes in universities/research centers.

METHODOLOGY

The simulations were done using PHITS (Particle and Heavy Ion Transport-code System) version 3.30 developed and distributed by Japanese Atomic Energy Agency (JAEA). PHITS is a multipurpose Monte Carlo software which can simulate and calculated the transport of both charged and uncharged particles across broad energy range (Sato *et al.*, 2023) [13].

The model consists of an air-filled room with size 1.8 m x 1.8 m x 3 m with 20 cm of concrete wall as the boundary. At the center of the room is a D-D generator, working at the flux of 5 x 10^9 fast neutrons every second. The neutrons are monoenergetic (2.45 MeV) and are radiated isotropically from the bottom of the tube, which is assumed to be cylindrical in shape (d = 7 cm, h = 5 cm). The neutron tube is surrounded by high-density polyethylene (C_2H_4) moderator in the shape of quasi-octagonal shape, 90 cm in diameter. This shape is chosen so that many beam tubes can be installed on it. Within the moderator there are several holes as the irradiation chambers, each with the dimension of 10 cm x 10 cm x 10 cm filled with air. The center coordinate of each irradiation chamber within the moderator is tabulated in Table 1.

Table 1. Center position of source and irradiation chambers

Cell	y (cm)	z (cm)	Distance from source (cm)
Source	0	45	-
A	0	20	25
B_1	20	20	32.02
B_2	-20	20	32.02
C_1	20	45	20
C_2	-20	45	20
D_1	20	70	32.02
D_2	-20	70	32.02
E_1	20	95	53.85
E_2	-20	95	53.85

The moderator also surrounds the guide tube, which is 10 cm x 10 cm in cross section. The guide tube is placed either radially or tangentially. It is about 90-cm long and consists of silica (SiO_2) wall with alternating nickel-titanium thin layers to reflect the neutrons inside the tube. The thin layers are 200-nm thick each and there are 75 layers of it, which together they form a 15-μm thick super mirror layer. A super mirror usually consists of thin layers of two different materials deposited on top of the other, with one material has high neutron optical potential and the other has low neutron optical potential [14]. Nickel and titanium are chosen for the large contrast of their scattering length density [15]. The configurations of the moderator, together with the cavities and the guide tube are shown in Figure 2-6.

The tally used in the simulation is [T-Track] and [T-Cross]. Tally [T-Track] are used to illustrate the trajectories of the neutrons and the energy range of the neutrons in the activation chambers. The fluence on the end of the guide tube is done using [T-Cross], as it calculates the fluence of particles crossing any surface. The energy range is divided into three categories: the thermal region (0.001-0.1 eV); the epithermal region (0.1 eV – 10 keV); and the fast region (above 10 keV).

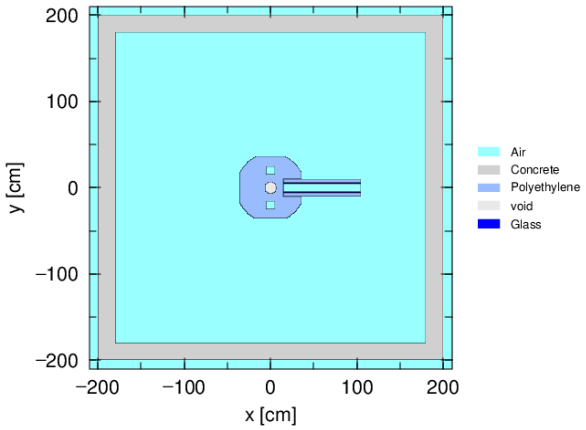

Fig. 2. Top view of simulated region with radial beam tube

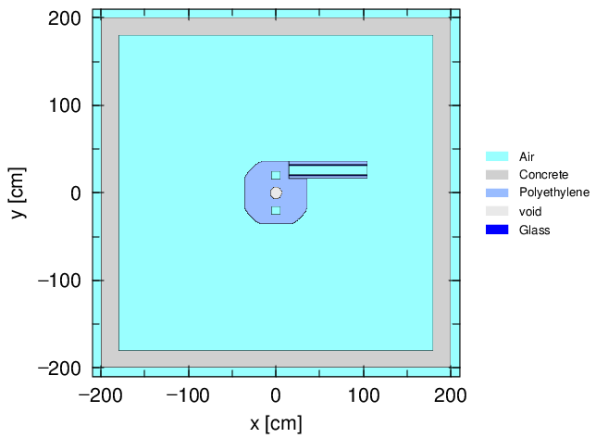

Fig. 3. Top view of simulated region with tangential beam tube

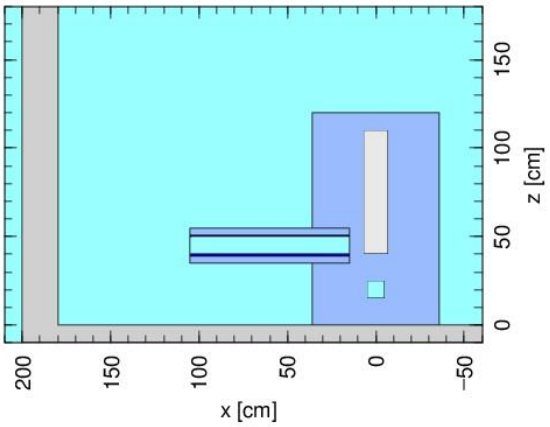

Fig. 4. Moderator and beam tube from the side view

RESULTS AND DISCUSSION

Table 2 tabulates the fluence of neutrons within the irradiation cavities in terms of energy and Figure 7 shows the comparison of thermal flux in the chambers. The difference between cells arranged on the same height (for instance, B_1 and B_2) is small compared to the relative error so it can be deduced that those two data are not significantly different and thus are treated as the same data. As the cells are arranged symmetrically, the fluences are only mentioned once for convenience purpose.

The chamber numbered C_1 and C_2 have the biggest fluence overall, with 63% of neutrons being in the thermal region (see Table 3). Over 1.95 x 10^9 thermal neutrons traversed these two cells. These two chambers are the closest ones to the source hence the number of neutrons is the highest, as can be seen in Table 1. As the distance from the neutron source grows, the fluence diminishes as the neutrons are spread out to bigger area. Meanwhile, the thermal contribution in the cell C_1 and C_2 is the lowest. Since those cells are the closest one to the source, large percentage of neutrons enters the irradiation cavities without being properly slowed down. This also explains that the large fluence of fast neutrons in the cell C_1 and C_2 happens due to incomplete thermalization.

The next cell with biggest thermal flux is the cell A, which is located 25 cm below the source. These extra few centimeters, compared to cells C_1 and C_2, provide enough moderation to suppress the fast neutrons (12.04% vs 18.32%) and enhance the thermalization process (70.91% vs 63.00%). The cells B_1 and B_2, although separated by the same distance from the source as the cells D_1 and D_2, have larger thermal neutron and fewer fast neutrons flux. This can be explained that the neutron generator tube consists of short linear accelerator which must be kept vacuum. Therefore, the neutrons coming into cells D_1 and D_2 encounter less moderation due to this vacuum tube. On the other hand, the neutrons entering cells B_1 and B_2 have travelled through more HDPE moderator and thus more moderated. The cells E_1 and E_2, which are farthest out from the source and thus get the smallest fluence, have over 4.0 x 10^7 thermal neutrons within the cells, which is enough for activation experiment. The fast neutrons only comprise 5.07% of all neutrons coming into cells E_1 and E_2, indicating that the thermalization is nearly complete. Of all irradiation chambers, fast neutrons comprise no more than 20% of all neutrons travelling through the chambers. This indicates the efficiency of high-density polyethylene in moderating fast neutrons [16-17].

Table 2. Neutron fluence in the activation chambers by energy (1/(cm^2.s))

Cell	Thermal (10^{-3} – 10^{-1} eV)	Epithermal (10^{-1} – 10^{4} eV)	Fast (>10 keV)
A	5.74 x 10^8 ± 0.60%	1.38 x 10^8 ± 0.96%	9.75 x 10^7 ± 1.17%
$B_{1,2}$	1.25 x 10^8 ± 1.24%	2.65 x 10^7 ± 2.11%	1.71 x 10^7 ± 2.84%
$C_{1,2}$	1.95 x 10^9 ± 0.34%	5.78 x 10^8 ± 0.49%	5.67 x 10^8 ± 0.48%
$D_{1,2}$	3.34 x 10^8 ± 0.78%	7.71 x 10^7 ± 1.27%	5.54 x 10^7 ± 1.59%
$E_{1,2}$	4.08 x 10^7 ± 2.11%	7.50 x 10^6 ± 3.74%	2.58 x 10^6 ± 7.15%

Table 3. Neutron energy percentage in the activation chambers

Cell	Thermal (10^{-3} – 10^{-1} eV)	Epithermal (10^{-1} – 10^{4} eV)	Fast (>10 keV)
A	70.91%	17.05%	12.04%
$B_{1,2}$	74.14%	15.72%	10.14%
$C_{1,2}$	63.00%	18.68%	18.32%
$D_{1,2}$	71.60%	16.53%	11.88%
$E_{1,2}$	80.19%	14.74%	5.07%

Figure 8 illustrate the spatial distribution of neutrons in the room with radial beam tube while Figure 9 displays the energy distribution at the end of the radial beam tube. It can be seen that there are more neutrons travelling inside the beam tube than outside the tube. From the spectrum in Figure 9, the neutron energy has a peak in the thermal region at energy about 33.5 eV. This is not high peak however, as it contains only 2.08 x 10^2 neutrons/(cm^2.s). For an experiment with high monoenergetic flux requirement such as elastic scattering, this number is too low compared to for example the BRIN small angle scattering facility (SN2-NGH) which can irradiate sample with approximately 4.0 x 10^6 neutrons/(cm^2.s) [18]. In addition, this peak is dwarfed by the number of neutrons fast neutrons, which stands at 4.1 x 10^3 neutrons/(cm^2.s) at energy 2.45 MeV.

Figure 10 shows the spatial distribution of neutrons in the room with tangential beam tube while Figure 11 reveals the energy distribution at the end of the tangential beam tube. It shows that the fluence of neutrons in the tube is not as high as in the Figure 8 and Figure 9. As such, the thermal peak is even lower with only 49 neutrons/(cm^2.s) in the energy about 39 eV. On the other hand, it can be seen from Figure 11 that the fast neutron peak on the far-right side is no longer there, suggesting that tangential configuration is capable to suppress the number of fast neutrons along the tube.

In terms of total neutrons transported by the beam tube, the radial beam tube transports more neutrons than the tangential one. The radial beam tube delivers 2.06 x 10^4 neutrons/(cm^2.s) of which 38.15% of them are in the thermal region. On the other hand the tangential beam tube delivers 2.53 x 10^3 neutrons/(cm^2.s) and 73.23% of them are thermal. The numbers of thermal neutrons transported in these two designs are comparable to simulations done by Bergaoui et al. (2014) who reported thermal flux in the range of 2 x 10^2 up to 3 x 10^4 from a generator with 10^{10} maximum yield [6]. It is also matched the flux given by other accelerator-based neutron sources such as those belong to PKUNIFTY, INEST, or RIKEN [8,19-20].

Table 4. Neutron energy spectrum and gamma fluence on the end of the beam tube

Categories	Radial (n/(cm^2.s))	Tangential (n/(cm^2.s))
Thermal (0.001 – 0.1 eV)	7.86 x 10^3 ± 3.39%	1.86 x 10^3 ± 4.13%
Epithermal (0.1 eV – 10^4 eV)	3.11 x 10^3 ± 4.67%	4.78 x 10^2 ± 9.49%
Fast (>10 keV)	9.60 x 10^3 ± 2.41%	2.00 x 10^2 ± 14.05%
Gamma rays	2.12 x 10^4 ± 2.47%	2.43 x 10^4 ± 2.47%

The DD generator works by projecting fast neutrons (E_0 = 2.45 MeV) to all direction. Those fast neutrons are then slowed down by HDPE moderator. In case of radial beam tube, due to the proximity of the source and the start of the beam tube, fast neutrons could escape without being moderated. As such, 45% of neutrons exiting radial beam tube are fast neutrons. This is evident from Figure 9 when the neutron energy spectrum is taken into account. The far-right part of the spectrum represents neutrons that are still on the initial energy (2.45 MeV). It means that those neutrons do not undergo any moderation. Furthermore, because these neutrons are ejected radially, they are already on the same direction as the beam tube. So, once they escape the moderator, they will travel along the beam tube unimpeded. This explains why many fast neutrons are being counted at the end of the radial beam tube.

On the contrary, the start of the beam tube in the tangential configuration lies farther from the source so the chance of moderation is higher. This also means that the fluence will be lower to begin with compared to radial beam tube. To enter the beam tube, neutrons must first come into contact with the HDPE moderator, since the direction of the beam tube makes an angle with the radial direction of fast neutrons (hence called tangential). This will make sure that the neutrons travelling along the beam tube are already slowed down. The slower the neutrons, the more chance they will be slowed down again, since the reaction cross section grows upward as the neutron energy decreases. This will further reduce the neutron energy until they reach thermal equilibrium. Therefore, only thermalized neutrons are transported and any fast neutron counted at the end of the tangential beam tube is most likely from the neutrons that exits the moderator, enters the guide tube from outside, and then crossing the calculated surface.

Neutrons that encounter alternating thin layers will undergo multiple transmission and reflection that result in interference of multiple neutron wave vectors. The super mirror works by reflecting neutrons that graze from less than its critical scattering vector (Q_c), which is proportional to its incoming angle and reciprocal to its wavelength. Thus, the reflectivity of certain neutron wave depends on its energy and lower neutron energy means greater critical angle [14-15]. Hence, the super mirror is more effective to reflect thermal neutrons than fast neutrons, which is another reason why the neutrons at the end of the tangential beam tube is mostly thermal.

CONCLUSION

Simulations have been conducted on the design of NAA facility and thermal radiography facilities based on DD generator. By having high-density polyethylene as moderator, high thermal flux from 4.08 x 10^7/(cm^2.s) up to 1.95 x 10^9/(cm^2.s) in the irradiation chambers can be achieved. Two radiography beam tubes have been simulated, with the radial beam tube transports 7.86 x 10^3/(cm^2.s) thermal neutrons, comprising about 38.15% of all neutrons. On the other hand, tangential beam tube transports 1.86 x 10^3/(cm^2.s) thermal neutrons, which is 73.23% of all neutrons coming at the end of the tube. This indicates the effectiveness of tangential configuration to suppress the number of fast neutrons, which is filtered by having neutron super mirror on the surface of the beam tube.

This research shows that high-flux DD generators (producing more than 5 x 10^9 neutrons/s) can be employed as a source for experiments with low fluence requirement such as NAA or radiography. The relatively low neutron energy will require less moderation compared to source with higher energy such as DT generators or Am-Be sources. The further redesigning of super mirror could also be investigated in the future research, as it has been proven to increase the number of neutrons passing the long beam tube.

ACKNOWLEDGMENT

This project is done thanks to grant from Research Organization for Nuclear Energy (ORTN – BRIN) number D1208. The author also thanks Mr. Kasmudin from ORTN for the use of institutional computer to speed up the simulation processes.

REFERENCES

[1] L. Wehmeyer, R. Radel, and G. L. Kulcinski, Optimizing Neutron Production Rates from D-D Fusion in an Inertial Electrostatic Confinement Device, *Fusion Sci. Tech.* **47**, 14, 2004.

[2] E. J. Mausolf *et al.*, Fusion-Based Neutron Generator Production of Tc-99m and Tc101: A Prospective Avenue to Technetium Theranostics, *Pharmaceuticals* **14**, 875, 2021.

[3] D. P. Gulo *et al.*, Desain Beam Shaping Assembly (BSA) Berbasis D-D Generator 2,45 MeV untuk Uji Fasilitas BNCT, *Indonesian J. App. Phys.* **5**, 25, 2015.

[4] T. Al-Abdullah *et al.*, Sulfur Analysis in Bulk Samples Using a DD Portable Neutron Generator Based PGNAA Setup, *J. Radioanal. Nucl. Chem.* **326**, 555, 2020.

[5] J. T. Cremer *et al.*, Large area imaging of hydrogenous materials using fast neutrons from a DD fusion generator, *Nucl. Instrum. Methods Phys. Res. A* **675**, 51, 2012.

[6] K. Bergaoui *et al.*, Design, Testing and Optimization of a Neutron Radiography System Based on a Deuterium–Deuterium (D–D) Neutron Generator, *J. Radioanal. Nucl. Chem.* **299**, 41, 2014.

[7] IAEA Radiation Technology Reports No. 1: Neutron Generators for Analytical Purposes, International Atomic Energy Agency (IAEA), 2012.

[8] Z. Guo *et al.*, Neutron Radiography with Compact Accelerator at Peking University: Problems and Solutions, *Phys. Procedia* **26**, 70, 2012.

[9] Report of a Consultancy Meeting: Nondestructive and Analytical Techniques Using Neutrons, 08CT14309, International Atomic Energy Agency (IAEA), 2019.

[10] D. L. Williams *et al.*, A Fast Neutron Radiography System Using a High Yield Portable DT Neutron Source, *J. Imag.*, **6**, 128, 2020.

[11] J. S. Brenizer, 7th Int. Topic. Meet. on Neutron Radiograpy (Jun 16-24, 2012, Kingston, Canada) vol 43 (Amsterdam: North-Holland/American Elsevier), 10, 2013.

[12] Y. Otake, RIKEN Accelerator-driven Compact Neutron Systems, RANS Projects, and Their Capabilities, *Neutron News* **2-4**, 32, 2021.

[13] T. Sato *et al.*, Recent Improvements of the Particle and Heavy Ion Transport-code System – PHITS version 3.33, *J. Nucl. Sci. Technol.*, 2023.

[14] K. Ikeda *et al.*, Development of Ni/Ti Supermirrors with Large *m* and a Curved Surface, *Nucl. Instrum. Methods Phys. Res. A* **529**, 78, 2004.

[15] S. Masalovich, Analysis and Design of Multilayer Structures for Neutron Monochromators and Supermirrors, *Nucl. Instrum. Methods Phys. Res. A* **722**, 71, 2013.

[16] J. Rataj *et al*., Characterisation of Neutron Field in the Polyethylene Neutron Irradiator, *J. App. Rad. Iso.* **168**, 109529, 2021.

[17] P. Gan *et al.*, Progress in commissioning a neutron/X-ray radiography and tomography systems at IAEA NSIL, *J. Instrumentation* **17**, 11001, 2022.

[18] E. G. R. Putra *et al.*, Proc. 13th Int. Conf. on Small-Angle Scattering (Jul. 9-13, 2006, Kyoto, Japan), vol 40 (International Union of Crystallography), 447, 2007.

[19] L. Zhang *et al.*, Resolution Analysis of Thermal Neutron Radiography Based on Accelerator‐driven Compact Neutron Source, *Nuc. Sci. Tech.* **34**, 76, 2023.

[20] Y. Kiyanagi, Neutron Imaging at Compact Accelerator-Driven Neutron Sources in Japan, *J. Imag.* **4**, 55, 2018.

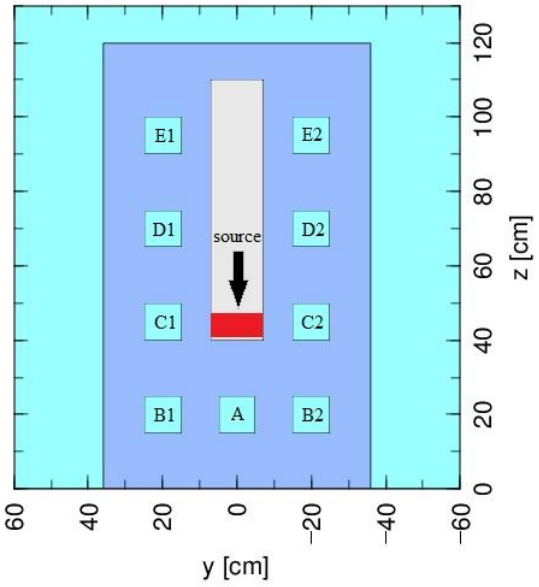

Fig. 5. Configuration of irradiation chambers within the moderator

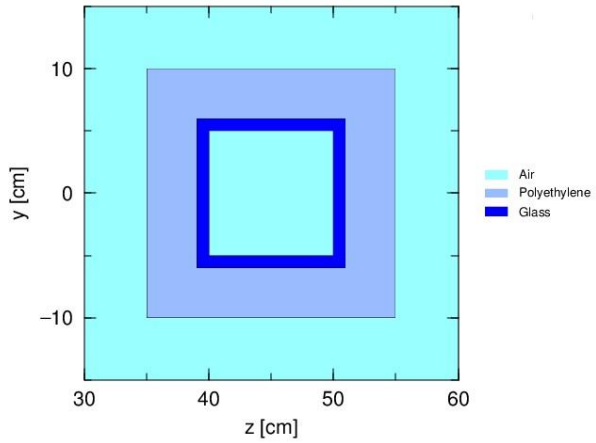

Fig. 6. Cross sectional view of the guide tube

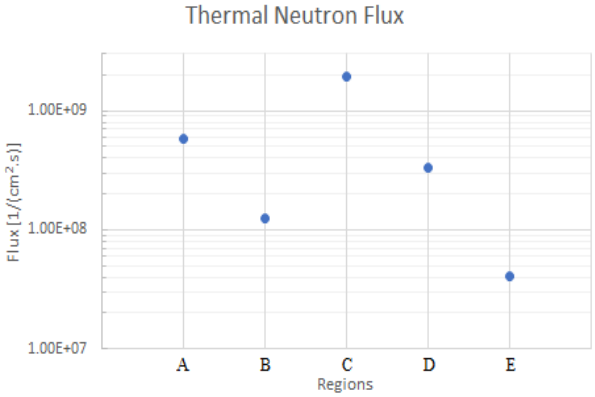

Fig. 7. Thermal neutron flux within the irradiation chambers

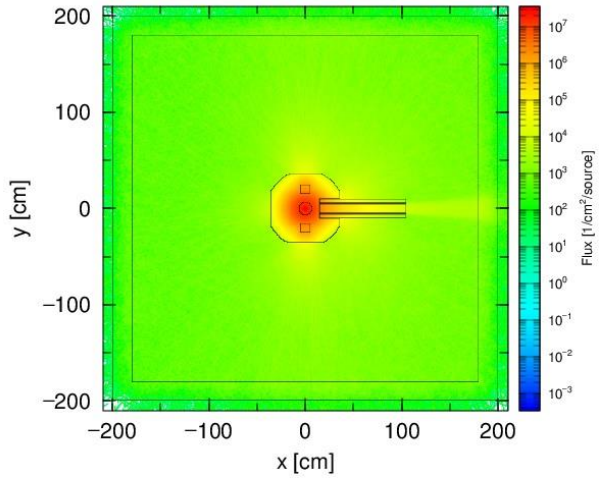

Fig. 8. Neutron distribution within the room with radial beam tube

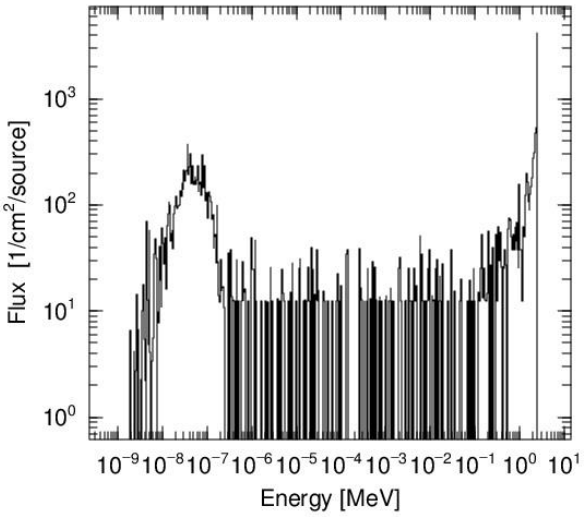

Fig. 9. Energy range from the neutrons exiting radial beam tube

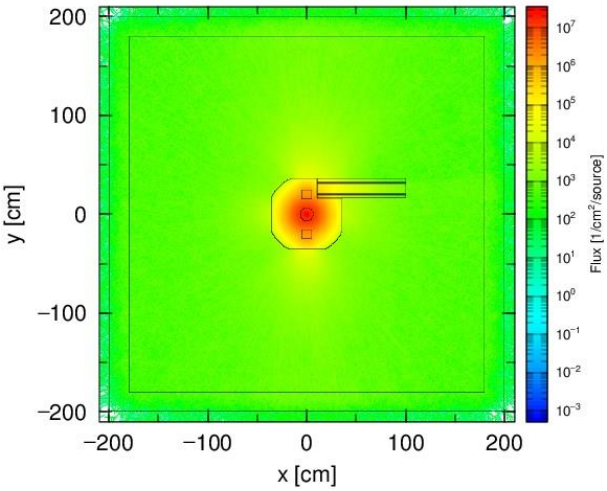

Fig. 10. Neutron distribution within the room with tangential beam tube

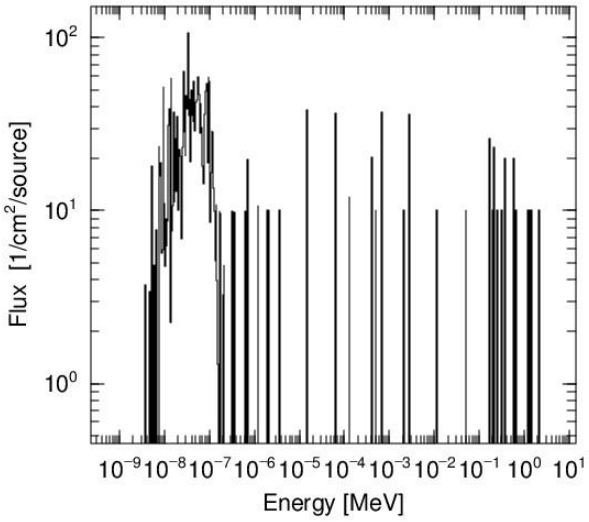

Fig. 11. Energy range from the neutrons exiting tangential beam tube